SURVEY AND LOGISTICS REPORT ON A HELICOPTER BORNE VERSATILE TIME DOMAIN ELECTROMAGNETIC (VTEM) SURVEY

on the

TASMANIA AREA

for

CORONA GOLD LIMITED

by

GEOTECH AIRBORNE PTY LTD

Unit 1, 29 Mulgul Road
Malaga, WA, 6090,
Australia
Tel: +61 8 9249 8814
Fax: +61 8 9249 8894
www.geotechairborne.com
e-mail: info@geotechairborne.com

Project AA895
June, 2011

TABLE OF CONTENTS

1. SURVEY SPECIFICATIONS 3
1.1. General 3
1.2. VTEM flight plan on Google EARTH™ Background 3
1.3. Survey block coordinates. 4
1.4. Survey block specifications 4
1.5. Survey schedule 5
2. SYSTEM SPECIFICATIONS 6
2.1. Instrumentation 6
2.2. VTEM Configuration 7
2.3. VTEM decay sampling scheme 7
2.4. VTEM Transmitter Waveform over one half-period (February 2011) 8
3. PROCESSING 9
3.1. Processing parameters 9
3.2. Flight Path 9
3.3. Electromagnetic Data 9
3.4. Magnetic Data 9
3.5. Digital Terrain Model 10
4. DELIVERABLES 11
5. PERSONNEL 13

APPENDICES

A. Modeling VTEM data 14
B. Geophysical Maps 20

SURVEY AND LOGISTICS REPORT ON A HELICOPTER-BORNE VTEM SURVEY

1. SURVEY SPECIFICATIONS

1.1. General

Job Number	AA895
Client	Corona Gold Limited
Project Area	Tasmania Area
Location	Australia
Number of Blocks	2
Total line kilometres	925km
Survey date	23 January – 7 March, 2011
Client Representative	Charles Hughes, Senior Geologist Tel: +61 894 864 482/ +64 439 813 780 Email: c.hughes@coronagold.net
Client address	Level 1, 703 Murray Street West Perth, 6005, Western Australia
SGC Consultant	Russell Mortimer Tel: +61 8 6254 5000 Fax: +61 8 6254 5099 Email: russell@sgc.com.au
SGC Address	Southern Geoscience Consultants Suite 1, Level 1, 183 Great Eastern Hwy Belmont. WA. 6104

1.2. VTEM flight plan on Google EARTH™ Background

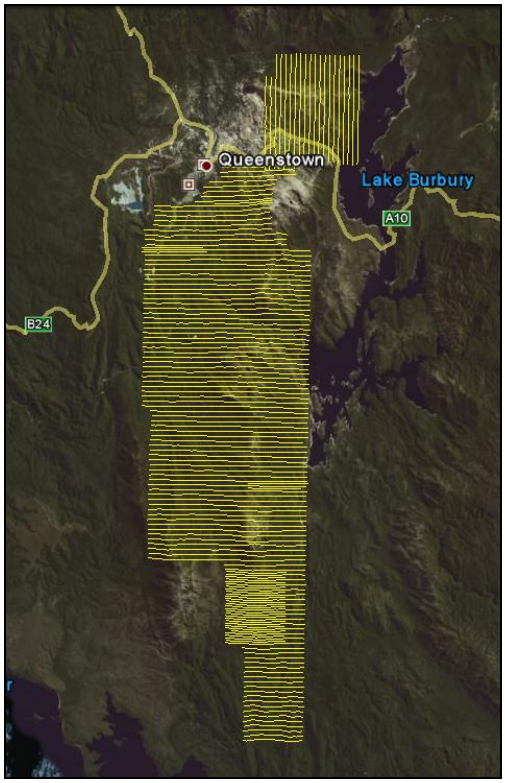

1.3. Survey block coordinates.

Easting UTM Z 55S	Northing UTM Z 55S
Block 1	
385994.136	5310984.77
385999.999	5336000
384744.271	5336140.55
384750.003	5336234.76
384750.003	5336734.76
383994.011	5336834.18
383994.024	5338749.4
384105.706	5338988.45
384105.697	5339496.4
385111.682	5339682.68
385105.753	5340250
382609.242	5340243.41
382609.25	5340476.35
382099.706	5340990.41
378994.057	5340990.41
378994.057	5340243.41
377994.059	5340004.38
377994.059	5337255.4
377501.04	5336996.66
377496.29	5328004.43
377991.198	5327729.43
377994.084	5320239.52
381994.085	5319985.7
381994.085	5315983.41
382994.108	5315734.78
382994.116	5310984
385994.136	5310984
Block 2	
385099.998	5340735
385105.753	5340100
383599.996	5340100
383596.302	5344782.16
384095	5344782.16
384095	5346000
388349.998	5346000
388349.998	5340500
386849.997	5340500
386717.555	5340735
385099.998	5340735
388349.998	5346000
388349.998	5340500
386849.997	5340500
386717.555	5340735

1.4. Survey block specifications

Survey block	Line spacing (m)	Line-km (contractual)	Line-km (delivered)	Flight direction	Line number
Block 1	250	849	815	090 – 270	L10010 – L12350
Block 2	250	N/A	111	000 - 180	L20010 – L20200

1.5. Survey schedule

Date	Flight #	Block	Nominal Production Km flown	Comments
23-Jan-11	1	2	40	Production
24-28 Jan – No production due to weather.				
29-Jan-11	2,3	2	71	Production
30 Jan – 1 Feb – No production due to weather.				
2-Feb-11	4,5	1	88	Production
3-8 Feb – No production due to Aircraft maintenance.				
9-Feb-11	6,7	1	84	Production
10-Feb-11	N/A	N/A	N/A	Bad weather
11-Feb-11	N/A	N/A	N/A	Bad weather
12-Feb-11	8-10	1	133	Production
13-Feb-11	11	1	0	Production
14-Feb-11	12-15	1	163	Production
15-Feb-11	16,17	1	122	Production
16-24 Feb – No production due to weather.				
25-Feb-11	18	1	36	Production
26 Feb – 3 Mar – No production due to weather.				
4-Mar-11	19	1	3	Production
5-Mar-11	20-22	1	203	Production
6-Mar-11	N/A	N/A	N/A	No Production
7-Mar-11	23	1	0	No Production

2. SYSTEM SPECIFICATIONS

2.1. Instrumentation

Survey Helicopter	
Model	AS 350 B3
Registration	VH-VTX
Nominal survey speed	80 km/h
Nominal terrain clearance	80 m
VTEM Transmitter	
Coil diameter	26 m
Number of turns	4
Pulse repetition rate	25 Hz
Peak current	200 Amp
Duty cycle	42%
Peak dipole moment	425,000 NIA
Pulse width	8.33 ms
Nominal terrain clearance	48 m
VTEM Receiver	
Coil diameter	1.2 metre
Number of turns	100
Effective area	113.1 m^2
Sampling interval	0.1 s
Nominal terrain clearance	48 m
Magnetometer	
Type	Geometrics
Model	Optically pumped cesium vapour
Sensitivity	0.02 nT
Sampling interval	0.1 s
Cable length	13 m
Nominal terrain clearance	71 m
Radar Altimeter	
Type	Terra TRA 3000/TRI 40
Position	Beneath cockpit
Sampling interval	0.2 s
GPS navigation system	
Type	NovAtel
Model	WAAS enabled OEM4-G2-3151W
Antenna position	Helicopter tail
Sampling interval	0.2 s
Base Station Magnetometer/GPS	
Type	Geometrics
Model	Cesium vapour
Sensitivity	0.001 nT
Sampling interval	1 s

2.2. VTEM Configuration

Configuration	
Cable angle with vertical	40 ˚
Cable length (EM receiver)	41 m
Cable length (Magnetometer)	11 m

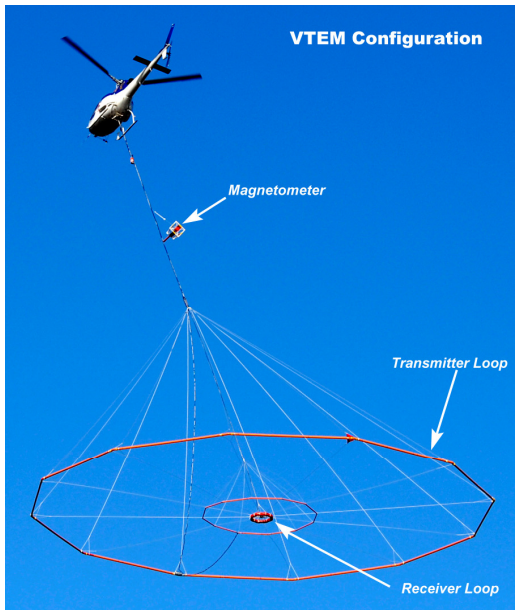

2.3. VTEM decay sampling scheme

B-field VTEM Decay Sampling scheme				
Array	Microseconds			
Index	Middle	Start	End	Width
13	83	78	90	12
14	96	90	103	13
15	110	103	118	15
16	126	118	136	18
17	145	136	156	20
18	167	156	179	23
19	192	179	206	27
20	220	206	236	30
21	253	236	271	35
22	290	271	312	40
23	333	312	358	46
24	383	358	411	53
25	440	411	472	61
26	505	472	543	70
27	580	543	623	81
28	667	623	716	93
29	766	716	823	107
30	880	823	945	122
31	1010	945	1086	141
32	1161	1086	1247	161
33	1333	1247	1432	185
34	1531	1432	1646	214
35	1760	1646	1891	245
36	2021	1891	2172	281
37	2323	2172	2495	323
38	2667	2495	2865	370
39	3063	2865	3292	427
40	3521	3292	3781	490
41	4042	3781	4341	560
42	4641	4341	4987	646
43	5333	4987	5729	742
44	6125	5729	6581	852
45	7036	6581	7560	979
46	8083	7560	8685	1125
47	9286	8685	9977	1292

2.4. VTEM Transmitter Waveform over one half-period (February 2011)

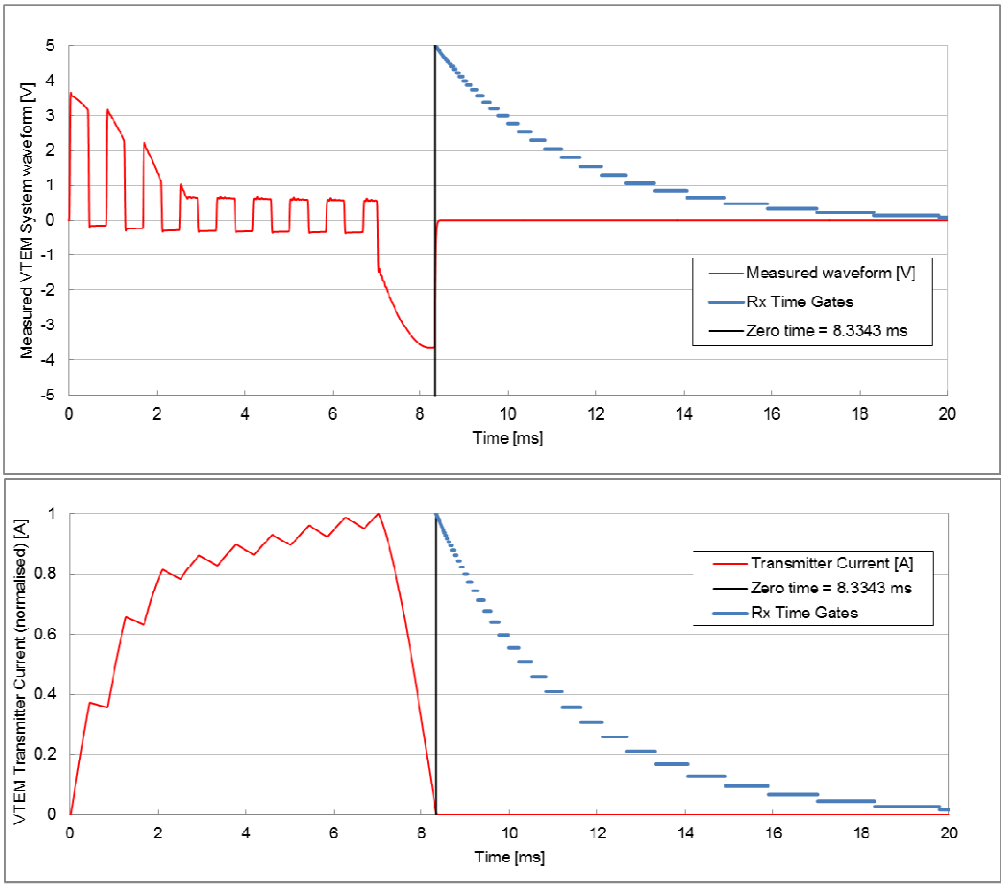

3. PROCESSING

3.1. Processing parameters

Coordinates	
Projection	MAP GRID AUS ZONE 55
Datum	GDA 94
Spherics rejection (EM and Magnetic data)	
Non-linear filter	4 point
Non-linear filter sensitivity	0.0001
Low-pass filter wavelength	15 fids
Lag correction of other sensors to EM receiver position	
GPS	19 m
Radar	29 m
Magnetometer	19 m

3.2. Flight Path

The flight path, recorded by the acquisition program as WGS 84 latitude/longitude, was converted into the UTM coordinate system in Oasis Montaj. The flight path was drawn using linear interpolation between x,y positions from the navigation system. Positions are updated every second and expressed as UTM eastings (x) and UTM northings (y).

3.3. Electromagnetic Data

A three stage digital filtering process was used to reject major sferic events and to reduce system noise. Local sferic activity can produce sharp, large amplitude events that cannot be removed by conventional filtering procedures. Smoothing or stacking will reduce their amplitude but leave a broader residual response that can be confused with geological phenomena. To avoid this possibility, a computer algorithm searches out and rejects the major sferic events.

The signal to noise ratio was further improved by the application of a low pass linear digital filter. This filter has zero phase shift which prevents any lag or peak displacement from occurring, and it suppresses only variations with a wavelength less than the specified filter wavelength.

3.4. Magnetic Data

The processing of the magnetic data involved the correction for diurnal variations by using the digitally recorded ground base station magnetic values. The base station magnetometer data was edited and merged into the Geosoft GDB database on a daily basis. The aeromagnetic data was corrected for diurnal variations by subtracting the observed magnetic base station deviations.

A micro-levelling procedure was then applied. This technique is designed to remove persistent low-amplitude components of flight-line noise.

The corrected magnetic data was interpolated between survey lines using a random point gridding method to yield x-y grid values for a standard grid cell size of a quarter of the line spacing. The Minimum Curvature algorithm was used to interpolate values onto a rectangular regular spaced grid.

3.5. Digital Terrain Model

Subtracting the radar altimeter data from the GPS elevation data creates a digital elevation model.

4. DELIVERABLES

VTEM Survey and logistics report		
Format	PDF	
Copies	2 x Digital (DVD/CD) 2 x Hard copy	
Database		
Format	Digital Geosoft (.GDB)	
Channels	Name	Description
	X_UTM	X positional data (UTM Z55S / WGS84)
	Y_UTM	Y positional data (UTM Z55S / WGS84)
	X_MGA	X positional data (MGA Z55 / GDA94)
	Y_MGA	Y positional data (MGA Z55 / GDA94)
	Lon	Longitude data
	Lat	Latitude data
	Z	GPS antenna elevation (metres above sea level)
	Radar	Helicopter terrain clearance from radar altimeter (metres above ground level)
	RxAlt	EM Receiver and Transmitter terrain clearance (metres above ground level)
	DTM	Digital terrain model (metres)
	Gtime	UTC time (seconds of the day)
	MagTF	Raw Total Magnetic field data (nT)
	MagBase	Magnetic diurnal variation data (nT)
	MagDiu	Total Magnetic field diurnal variation and lag corrected data (nT)
	MagMicL	Microleveled Total Magnetic field data (nT)
	dBdtZ[13] to dBdtZ[47]	dB/dtZ, Time Gates 83 µs to 9286 µs ($pV/A/m^4$)
	BfieldZ[13] to BfieldZ[47]	BfieldZ, Time Gates 83 µs to 9286 µs ($pV*m/A/m^4$)
	PLM	Power line monitor

Grids		
Format	Digital Geosoft (.GRD and .GI)[1]	
Grids	Name	Description
	AA895_Mag	Total Magnetic field (nT)

Maps		
Format	Digital Geosoft (.MAP)	
Scale	1:35 000	
Maps	Name	Description
	AA895_Mag	Total Magnetic field colour contours
	AA895_dBdtZ_Log	VTEM dB/dt profiles, Time Gates 0.667 – 9.286 ms in linear - logarithmic scale
	AA895_BfieldZ_Log	VTEM B-field profiles, Time Gates 0.667 – 9.286 ms in linear - logarithmic scale

[1] A Geosoft .GRD file has a .GI metadata file associated with it, containing grid projection information.

Waveform		
Format	Digital Excel Spreadsheet (AA895_VTEM_Waveform.xls)	
Columns	Name	Description
	Time	Sampling rate interval, 5.208 µs
	Volt	Output voltage of the receiver coil (volt)
	Current	Transmitter current (normalised to 1A peak)

Google Earth Flight Path file	
Format	Google Earth AA895_FlightPath.kml
	Free version of Google Earth software can be downloaded from, *http://earth.google.com/download-earth.html*

5. PERSONNEL

Geotech Airborne Limited Personnel	
Operator / Crew chief	Dan Delaney / Leon Lovelock
Data Processing (Preliminary)	Pete Holbrook
Data Processing (Final) /Reporting	Matt Holbrook
Final data supervision	Malcolm Moreton Data Processing Manager (malcolm@geotechairborne.com)
Overall project management	Keith Fisk Managing Partner and Director (keith@geotechairborne.com)

APPENDIX A

GENERALIZED MODELING RESULTS OF THE VTEM SYSTEM (by Roger Barlow)

Introduction

The VTEM system is based on a concentric or central loop design, whereby, the receiver is positioned at the centre of a 26.1 metres diameter transmitter loop that produces a dipole moment up to 625,000 NIA at peak current. The wave form is a bi-polar, modified square wave with a turn-on and turn-off at each end. With a base frequency of 25 Hz, the duration of each pulse is approximately 7.5 milliseconds followed by an off time where no primary field is present.

During turn-on and turn-off, a time varying field is produced (dB/dt) and an electro-motive force (emf) is created as a finite impulse response. A current ring around the transmitter loop moves outward and downward as time progresses. When conductive rocks and mineralization are encountered, a secondary field is created by mutual induction and measured by the receiver at the centre of the transmitter loop.

Measurements are made during the off-time, when only the secondary field (representing the conductive targets encountered in the ground) is present.

Efficient modeling of the results can be carried out on regularly shaped geometries, thus yielding close approximations to the parameters of the measured targets. The following is a description of a series of common models made for the purpose of promoting a general understanding of the measured results.

Variation of Plate Depth

Geometries represented by plates of different strike length, depth extent, dip, plunge and depth below surface can be varied with characteristic parametres like conductance of the target, conductance of the host and conductivity/thickness and thickness of the overburden layer.

Diagrammatic models for a vertical plate are shown in figures A and G at two different depths, all other parametres remaining constant. With this transmitter-receiver geometry, the classic **M** shaped response is generated. Figure A shows a plate where the top is near surface. Here, amplitudes of the duel peaks are higher and symmetrical with the zero centre positioned directly above the plate. Most important is the separation distance of the peaks. This distance is small when the plate is near surface and widens with a linear relationship as the plate (depth to top) increases. Figure G shows a much deeper plate where the separation distance of the peaks is much wider and the amplitudes of the channels have decreased.

Variation of Plate Dip

As the plate dips and departs from the vertical position, the peaks become asymmetrical. Figure B shows a near surface plate dipping 80º. Note that the direction of dip is toward the high shoulder of the response and the top of the plate remains under the centre minimum.

As the dip increases, the aspect ratio (Min/Max) decreases and this aspect ratio can be used as an empirical guide to dip angles from near 90º to about 30º. The method is not sensitive enough where dips are less than about 30º. Figure E shows a plate dipping 45º and, at this angle, the minimum shoulder starts to vanish. In Figure D, a

flat lying plate is shown, relatively near surface. Note that the twin peak anomaly has been replaced by a symmetrical shape with large, bell shaped, channel amplitudes which decay relative to the conductance of the plate.

Figure H shows a special case where two plates are positioned to represent a synclinal structure. Note that the main characteristic to remember is the centre amplitudes are higher (approximately double) compared to the high shoulder of a single plate. This model is very representative of tightly folded formations where the conductors where once flat lying.

Variation of Prism Depth

Finally, with prism models, another algorithm is required to represent current on the plate. A plate model is considered to be infinitely thin with respect to thickness and incapable of representing the current in the thickness dimension. A prism model is constructed to deal with this problem, thereby, representing the thickness of the body more accurately.

Figures C, F and I show the same prism at increasing depths. Aside from an expected decrease in amplitude, the side lobes of the anomaly show a widening with deeper prism depths of the bell shaped early time channels.

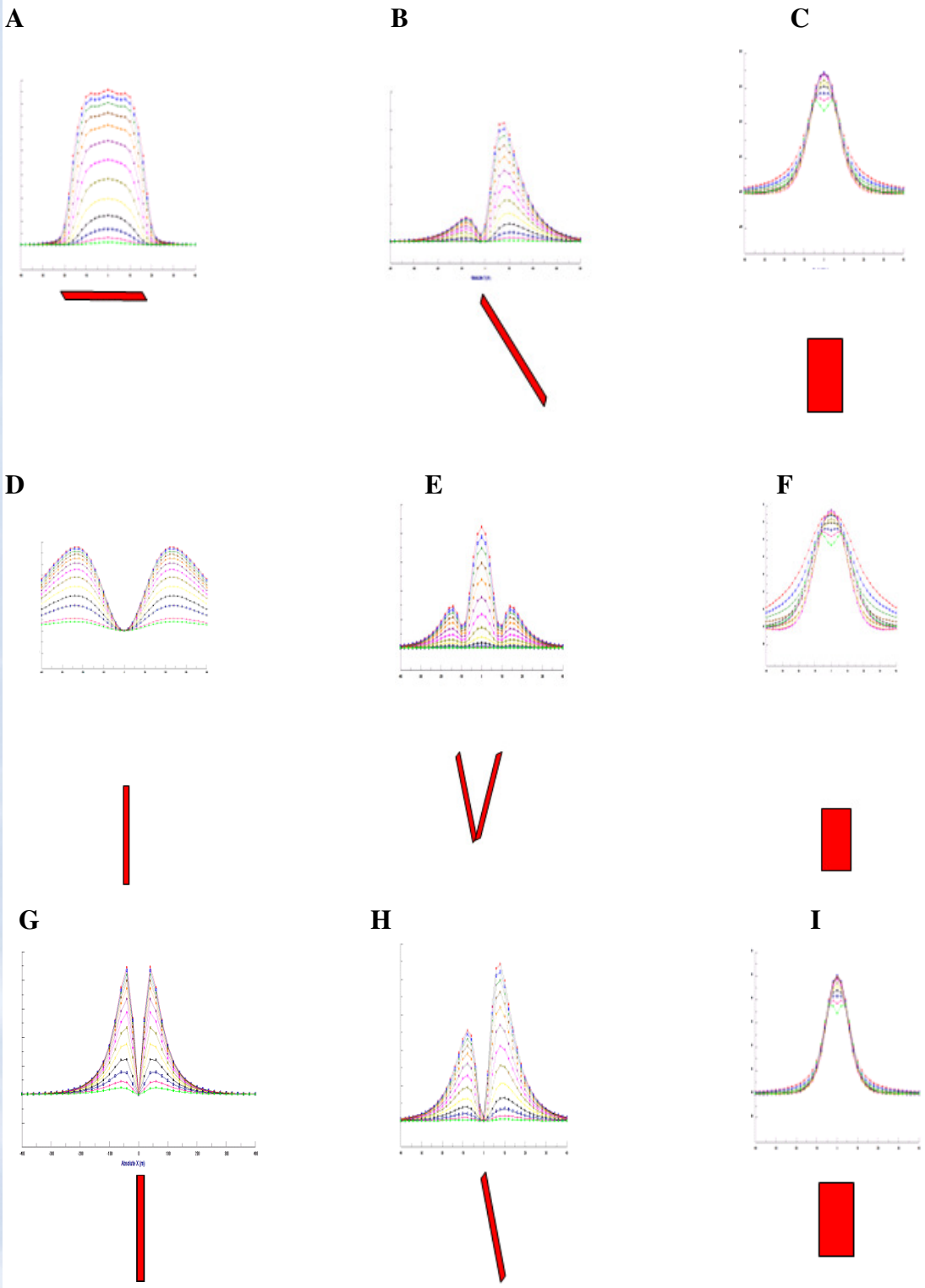
A
B
C
D
E
F
G
H
I

General Modeling Concepts

A set of models has been produced for the Geotech VTEM® system with explanation notes (see models A to I above). The reader is encouraged to review these models, so as to get a general understanding of the responses as they apply to survey results. While these models do not begin to cover all possibilities, they give a general perspective on the simple and most commonly encountered anomalies.

When producing these models, a few key points were observed and are worth noting as follows:

- For near vertical and vertical plate models, the top of the conductor is always located directly under the centre low point between the two shoulders in the classic **M** shaped response.
- As the plate is positioned at an increasing depth to the top, the shoulders of the **M** shaped response, have a greater separation distance.
- When faced with choosing between a flat lying plate and a prism model to represent the target (broad response) some ambiguity is present and caution should be exercised.
- With the concentric loop system and Z-component receiver coil, virtually all types of conductors and most geometries are most always well coupled and a response is generated (see model H). Only concentric loop systems can map this type of target.

The modelling program used to generate the responses was prepared by PetRos Eikon Inc. and is one of a very few that can model a wide range of targets in a conductive half space.

General Interpretation Principals

Magnetics

The total magnetic intensity responses reflect major changes in the magnetite and/or other magnetic minerals content in the underlying rocks and unconsolidated overburden. Precambrian rocks have often been subjected to intense heat and pressure during structural and metamorphic events in their history. Original signatures imprinted on these rocks at the time of formation have, it most cases, been modified, resulting in low magnetic susceptibility values.

The amplitude of magnetic anomalies, relative to the regional background, helps to assist in identifying specific magnetic and non-magnetic rock units (and conductors) related to, for example, mafic flows, mafic to ultramafic intrusives, felsic intrusives, felsic volcanics and/or sediments etc. Obviously, several geological sources can produce the same magnetic response. These ambiguities can be reduced considerably if basic geological information on the area is available to the geophysical interpreter.

In addition to simple amplitude variations, the shape of the response expressed in the wave length and the symmetry or asymmetry, is used to estimate the depth, geometric parameters and magnetization of the anomaly. For example, long narrow magnetic linears usually reflect mafic flows or intrusive dyke features. Large areas with complex magnetic patterns may be produced by intrusive bodies with significant magnetization, flat lying magnetic sills or sedimentary iron formation. Local isolated circular magnetic patterns often represent plug-like igneous intrusives such as kimberlites, pegmatites or volcanic vent areas.

Because the total magnetic intensity (TMI) responses may represent two or more closely spaced bodies within a response, the second derivative of the TMI response may be helpful for distinguishing these complexities. The second derivative is most useful in mapping near surface linears and other subtle magnetic structures that are partially masked by nearby higher amplitude magnetic features. The broad zones of higher magnetic amplitude, however, are severely attenuated in the vertical derivative results. These higher amplitude zones reflect rock units having strong magnetic susceptibility signatures. For this reason, both the TMI and the second derivative maps should be evaluated together.

Theoretically, the second derivative, zero contour or colour delineates the contacts or limits of large sources with near vertical dip and shallow depth to the top. The vertical gradient map also aids in determining contact zones between rocks with a susceptibility contrast, however, different, more complicated rules of thumb apply.

Concentric Loop EM Systems

Concentric systems with horizontal transmitter and receiver antennae produce much larger responses for flat lying conductors as contrasted with vertical plate-like conductors. The amount of current developing on the flat upper surface of targets having a substantial area in this dimension, are the direct result of the effective coupling angle, between the primary magnetic field and the flat surface area. One therefore, must not compare the amplitude/conductance of responses generated from flat lying bodies with those derived from near vertical plates; their ratios will be quite different for similar conductances.

Determining dip angle is very accurate for plates with dip angles greater than 30º. For angles less than 30º to 0º, the sensitivity is low and dips can not be distinguished accurately in the presence of normal survey noise levels.

A plate like body that has near vertical position will display a two shoulder, classic **M** shaped response with a distinctive separation distance between peaks for a given depth to top.

It is sometimes difficult to distinguish between responses associated with the edge effects of flat lying conductors and poorly conductive bedrock conductors. Poorly conductive bedrock conductors having low dip angles will also exhibit responses that may be interpreted as surfacial overburden conductors. In some situations, the conductive response has line to line continuity and some magnetic correlation providing possible evidence that the response is related to an actual bedrock source.

The EM interpretation process used, places considerable emphasis on determining an understanding of the general conductive patterns in the area of interest. Each area has different characteristics and these can effectively guide the detailed process used.

The first stage is to determine which time gates are most descriptive of the overall conductance patterns. Maps of the time gates that represent the range of responses can be very informative.

Next, stacking the relevant channels as profiles on the flight path together with the second vertical derivative of the TMI is very helpful in revealing correlations between the EM and Magnetics.

Next, key lines can be profiled as single lines to emphasize specific characteristics of a conductor or the relationship of one conductor to another on the same line. Resistivity Depth sections can be constructed to show the relationship of conductive overburden or conductive bedrock with the conductive anomaly.

APPENDIX B

GEOPHYSICAL MAP IMAGES
(not to scale)

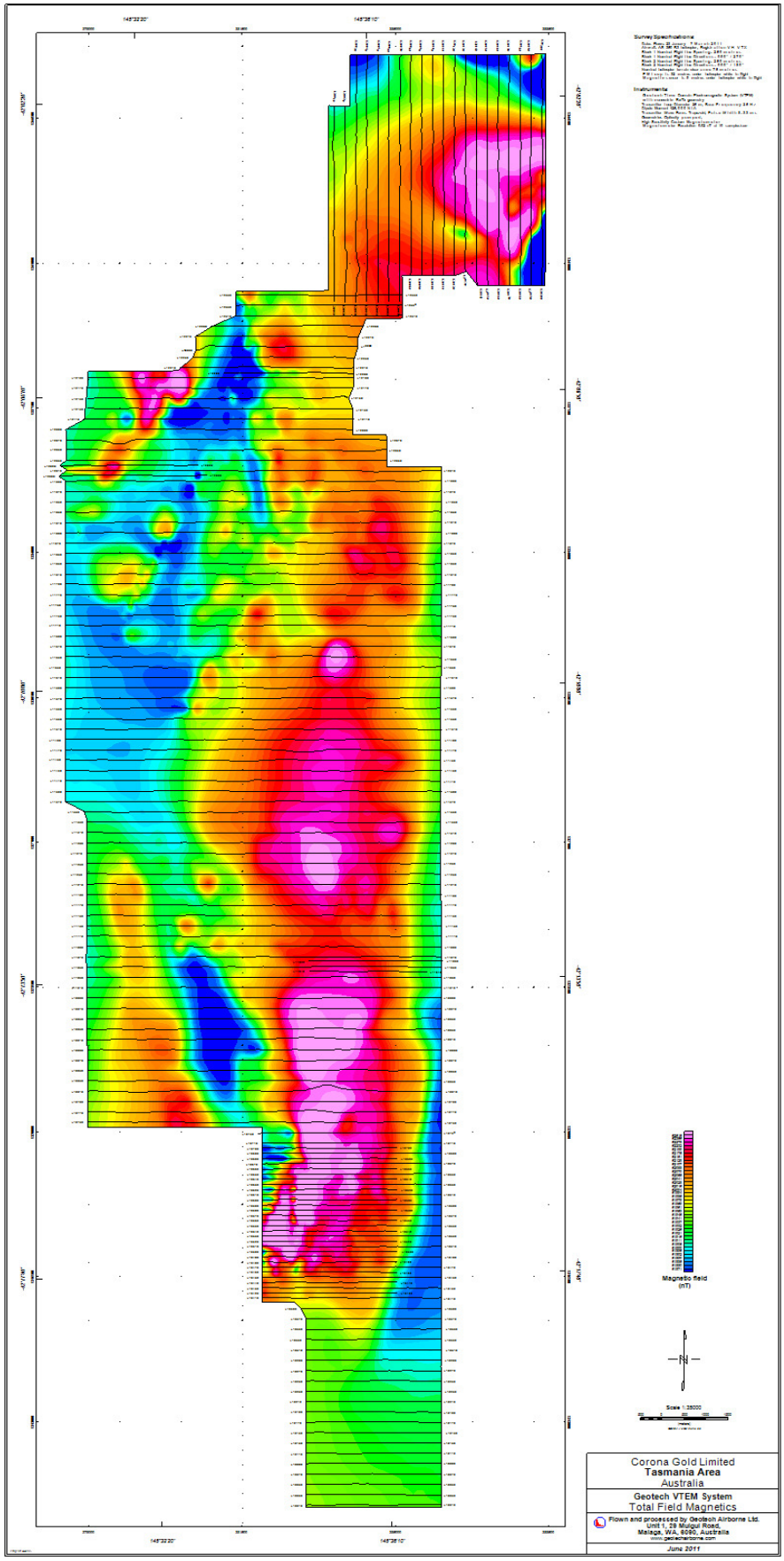
Survey Specifications
Instruments
Magnetic field
(nT)
Scale 1:25000
Corona Gold Limited
Tasmania Area
Australia
Geotech VTEM System
Total Field Magnetics
Flown and processed by Geotech Airborne Ltd.
Unit 1, 28 Mulgul Road,
Malaga, WA, 6090, Australia
www.geotechairborne.com
June 2011

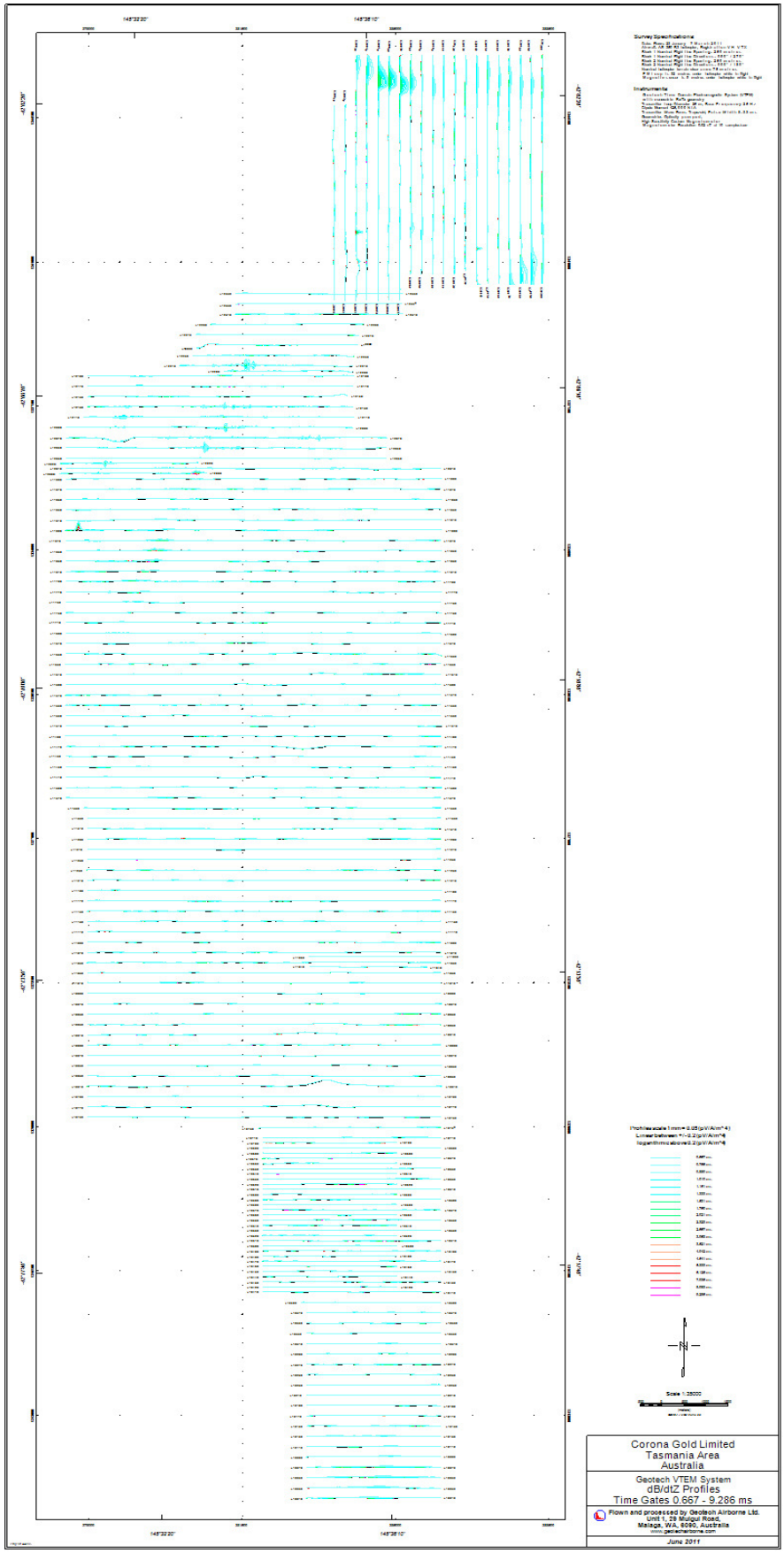
Corona Gold Limited
Tasmania Area
Australia
Geotech VTEM System
dB/dtZ Profiles
Time Gates 0.667 - 9.286 ms
Flown and processed by Geotech Airborne Ltd.
Unit 1, 29 Mulgul Road,
Malaga, WA, 6090, Australia
June 2011

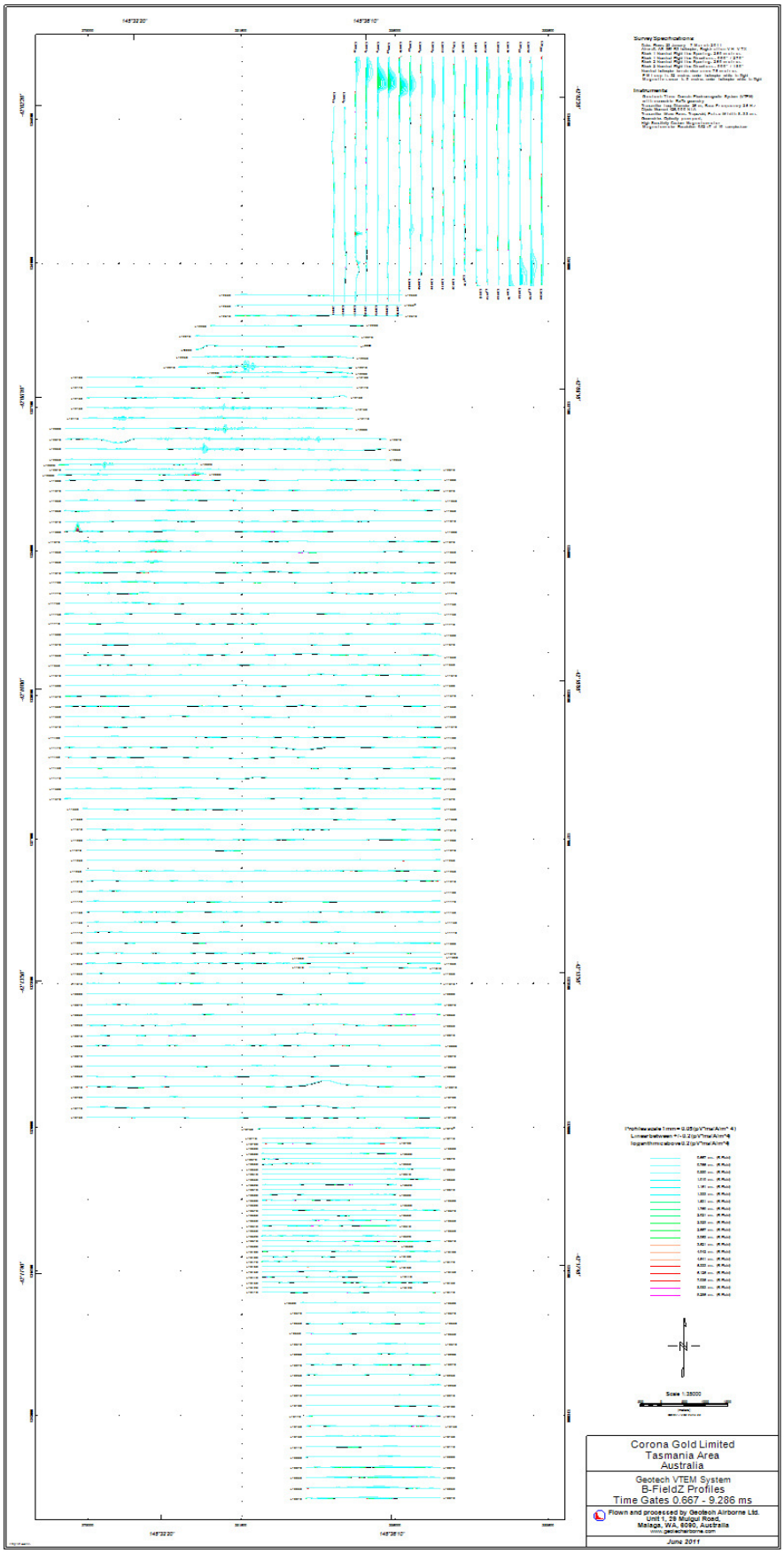
Corona Gold Limited
Tasmania Area
Australia
Geotech VTEM System
B-FieldZ Profiles
Time Gates 0.667 - 9.286 ms
Flown and processed by Geotech Airborne Ltd.
Unit 1, 28 Mulgul Road,
Malaga, WA, 6090, Australia
June 2011